

THE SYNTHESIS OF
BIMETALLIC
NANOPARTICLES USING
HUMAN CANCER CELLS

MIGUEL ANGEL ALVAREZ
SANCHEZ

NORTHEASTERN UNIVERSITY - UNIVERSITAT
ROVIRA I VIRGILI 2018

Contents

Acknowledgements	0
1. Objectives	1
2. Introduction	2
2.1. The problem of cancer. Statistics, factors and current treatments.	2
2.2. Synthesis of metal nanoparticles. Physico-Chemical and green approaches.....	7
2.3. Interactions between metal nanoparticles and cancer cells.....	10
3. State of the art	12
3.1. Synthesis of metal nanoparticles using human cells.....	12
3.2. Applications of metal nanoparticles in cancer treatments.	13
3.3. Applications of metal nanoparticles in photothermal treatments.	15
4. Materials and Methods	17
4.1. Materials.	17
4.2. Synthesis of G-Au/Pt and G-Au/Pd nanoparticles.....	17
4.3. Synthesis of G-Au/Pt-Tr and G-Au/Pd-Tr nanoparticles.....	18
4.4. Transmission Electron Microscopy	19
4.5. Energy-dispersive X-Ray Spectroscopy analysis EDS)	20
4.6. UV-Vis Spectrophotometry Analysis	20
4.7. Cytotoxicity assays.	20
4.8. Determination of Reactive Oxygen Species.	21
4.9. Photothermal Treatment.	22
5. Results and discussion	23
5.1. Synthesis of bimetallic nanoparticles	23
5.2. Cytotoxicity studies in Human Dermal Fibroblasts and Glioblastoma cells. ...	30
5.3. Intracellular measure of reactive oxygen species	34
5.4. Photothermal therapy of Glioblastoma cells using G-Au/Pt nanoparticles.	35
6. Conclusions and future prospects	38
6.1. Conclusions.....	38
6.2. Future prospects	39
7. References	40

Acknowledgements

- In the first place, thank you to my parents Miguel Angel and Angela, my sister Rebeca and the rest of my family for always staying there me and wishing the best for my life. I would have never fulfilled this adventure without you. Distance is hard, but it makes it easier with your support.
- In the second place, thank you to Prof Thomas J. Webster and Northeastern University for giving me the opportunity and accepting me as a member of the Nanomedicine group, and for all the support during these six months. Also thank you to all the Webster nanomedicine lab members, especially to Nicole Bassous and Kanny Chang for helping me with a part of the characterization, I wish you the best in your future. Also, thank you Ehsan Shirzaei and Andrew Spencer for allowing me to use their optical microscope and for all the help received.
- In the third place, thank you to the Spanish group: Lorena Baranda, Claudia Isern and Caterina Bartomeu for this amazing year together and for all the support we have had each other. This semester would have never been the same without you and thank you for teaching me the value of a good friendship. I am going to miss you so much.
- In the fourth place, thank you David Medina for letting me know about the Nanoscience master in Tarragona (Spain), and suggesting me to join Northeastern university to carry out my master thesis.
- In the fifth place, thank you to Bill Fowle for the trainings to use the TEM and SEM, but, most important, for his patience when thing went wrong in the measures. Especially, I want to mention in this section to Claudia again, for always supervising and staying with me when I went downstairs for hours. I owe you a big part of my TEM characterization.
- In the sixth place, I would like to thank Ian Harding and Jessica Fitzgerald from the writing center for all the comments in my master thesis and for helping me to express all my work in a clearer way.
- Finally, thank you to Courtney Pfluger and Joshua Gallaway for accepting to be part of my committee for my master thesis defense. I hope you enjoy reading this manuscript that collects all my effort during the last six months.

1. Objectives

Experimental goals:

- The main goal of this project is to synthesize and characterize different bimetallic nanoparticles via “green synthesis” using human cancer cells. This involves evaluating various methods of purification to determine the ideal method for isolating nanoparticles from the cellular matrix.
- Once the nanoparticles have been obtained and characterized, the second goal of the project is to evaluate their biocompatibility using healthy human cells (Human Dermal Fibroblasts) and anticancer properties in cancerous human cells. Specifically, the interactions between nanoparticles and cancer cells will be monitored.
- After studying the bio-characteristics of such metal nanoparticles, the third goal of this project is to evaluate the synthesized metal nanoparticles using a current cancer treatment, such as photothermal therapy, in an *in vitro* model.

2. Introduction

2.1. The problem of cancer. Statistics, factors and current treatments.

Cancer, which is characterized by the abnormal growth of tissue due to uncontrollable cells division, is one of the most harmful diseases worldwide. Over time, the progressive increase in the number of cell divisions and, subsequently, uncontrolled cell population growth, leads to the death of healthy cells surrounding the cancerous tissue. This can lead to tissue and organ failure and, eventually, death. Nowadays, there are more than 100 types of cancer that are classified by the type of cell they arise from, such as carcinomas from epithelial cells; leukaemia and lymphomas from blood and immune cells; or gliomas from brain tissue.¹ Within this last group, glioblastoma is the most common and aggressive malignant tumor in the primary central nervous system. It generally arises from glial cells, but also form from other cells types with neural stem cell-like properties. Additionally, glioblastomas typically appear in the brain (Fig 1.1 A) but have been reported in cerebellum or spinal cord. Lastly, they can appear at any age, including childhood, however, but are more common at older ages with a median age of 64 years.²

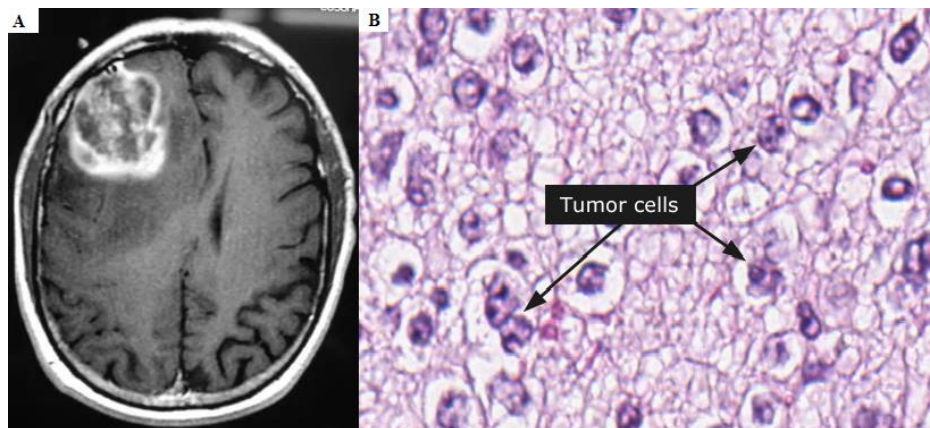


Figure 1.1. (A) Gadolinium-enhanced magnetic resonance of glioblastoma tumor in the frontal lobe.³ (B) Glioma from a neuroepithelial tissue.⁴

In 2016, almost two million patients were diagnosed with cancer in the United States, leading to 500,000 deaths. Furthermore, the cost of cancer treatments is estimated to exceed \$100 billion per year in the USA alone. More specifically, over 24,000 people were diagnosed with brain tumors in 2016, leading to 16000 deaths. This corresponds to 3% of total deaths caused by cancer.⁵

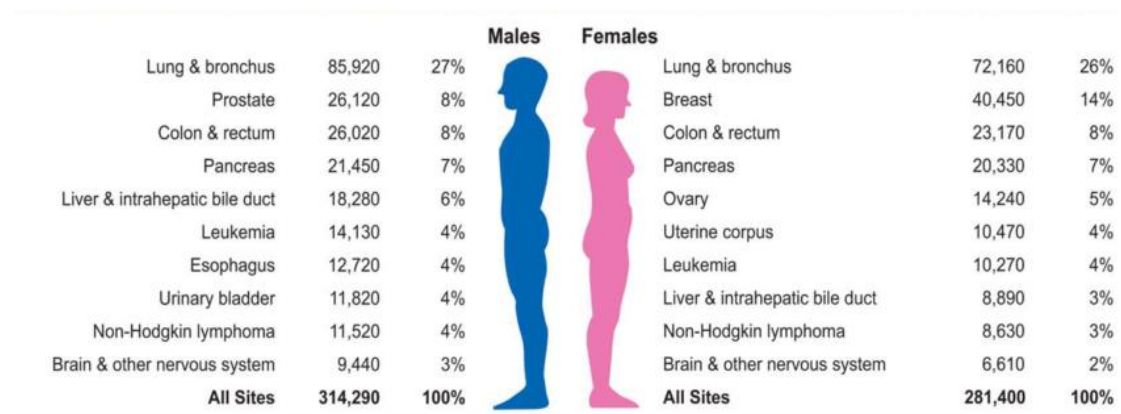


Figure 1.2. Estimated deaths from cancer in United States, 2016, excluding carcinomas.⁵

A variety of risk factors can contribute to the development of a tumor within biological tissue. For example, exposure to radiation (UV, x-rays),⁶ chemicals employed in (benzene, vinyl chloride),⁷ heavy air pollution⁸ or smoking⁹ are known to increase the risk of cancer development. Apart from these risk factors, some genetic diseases, such as neurofibromatosis, retinoblastoma have been found as potential risk factors for developing cancer, especially a glioblastomas.² Additionally, weight and diet are also two factors that can induce the development of cancer. Some aliments such as fats, processed food, alcohol or red meat have been reported to the risk of developing cancer if consumed in high quantities..¹⁰

The effectiveness and outcome of cancer treatments depends on both the patient and the cancer type.¹¹ In some scenarios, early diagnoses are essential to the success of

treatment. However, patients do not know the symptoms associated with cancer and can be misdiagnosed with other disease.¹² further hindering the success of cancer therapeutics. Aside from surgery, the most common cancer treatment,¹³ the most frequently used treatments are chemotherapy and radiation therapy.

Chemotherapy involves chemical drugs that are introduced intravenously or orally. Upon entering the bloodstream, they attack cancer cells, inducing cell apoptosis.¹⁴ One of the drugs most commonly used in chemotherapy is cisplatin, a metallic coordination compound of platinum (II) with planar geometry. It has the ability to crosslink with purine bases on cells' DNA structure, causing damage to cellular repair mechanisms and inducing cell apoptosis.¹⁵ However, these chemical drugs are often only effective towards a subset drug-sensitive cancer cells, as some cells develop resistance towards chemotherapeutics, resulting in increases metastasis.¹⁶

Radiotherapy, on the other hand, takes advantage of ionic radiation doses localized to tumors. These radiation doses produce DNA damage within the targeted area that leads to cell death.¹⁷ Usually, both chemotherapy and radiotherapy are used to improve the efficacy of treatment. However, they both contain significant limitations, such as varying effects on different patients and harmful side effects such as anaemia, organ damage, hair loss, and vomiting, among others.¹⁸ Additionally, when these techniques are ineffective, they are occasionally used as a palliative to reduce symptoms.¹⁹

Glioblastoma specifically can be treated by a variety of approaches that combine surgery with chemotherapy and a postoperative radiation therapy. Interestingly, the use of radiation therapy has been found to be more effective when used postoperatively than from the beginning of treatment; however, treatment success of glioblastomas has a

strong dependence on the size and shape of the tumor, and, more importantly, the area which it is located.²

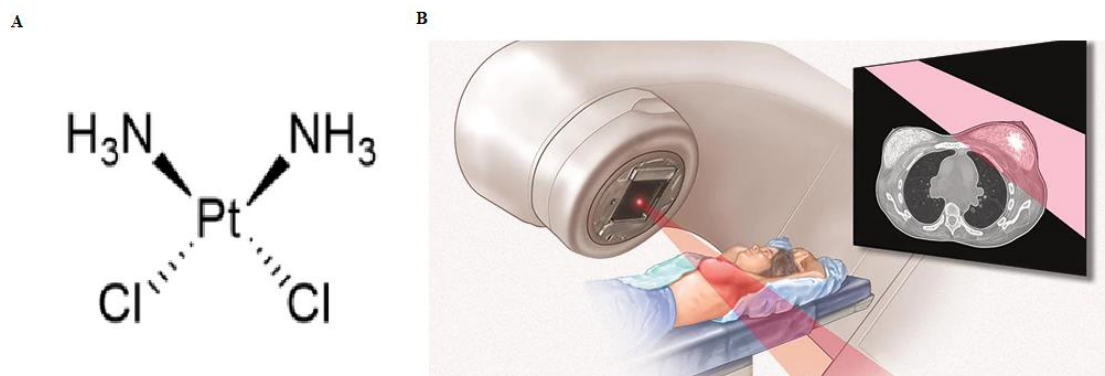


Figure 1.3. (A) Structure of Cisplatin, one of the most used drugs in chemotherapy treatments.²⁰ (B) Scheme of a Radiation therapy machine, where the radiation can be addressed specifically to the tumor location.²¹

Besides these common therapies, several new treatments have arisen in recent decades, such as immune therapy, hyperthermia, and gene therapy. Immune therapy is a technique that stimulates the natural defences in the human body. For this, antigens are introduced to stimulate the production of antibodies, (modifications in the immune system) that blocks proteins related to cancer cells. This technique has been found to be very successful; however, it is most often combined with chemotherapy or other therapies to increase its effectiveness.²²

In the case of hyperthermia, the treatment involves locally increasing temperature of tumor cells by using an external source, such as a magnetic field, which results in tumor cell death; although, the effectiveness of these techniques is not as good as is chemotherapy or radiotherapy.²³ Gene therapy, which consists of replacing damaged genes with their beneficial counterparts, has recently produced great results when

compared to traditional therapies. Unfortunately, the cost of this treatment is currently not affordable for most patients.²⁴

The use of nanotechnology for cancer treatment, which involves the use of particles with sizes between 1 and 100 nm, has recently gained influence as it is able to overcome some the current limitations of current cancer imaging techniques and drug delivery approaches.²⁵ For example, the physical properties of nanoparticles, such as shape, size, and surface to volume ratio, allow them to readily cross cell membranes.²⁶ Additionally, they can be modified to differentiate between cancer cells and healthy cells, which affords tumor targeting.²⁵

Additionally, photothermal therapy is a treatment that uses electromagnetic radiation to excite a photosensitizer, thereby increasing the temperature of these molecules and the surrounding tissue. When combined with nanotechnology, it represents a very promising technique. More specifically, nanoparticles that penetrate the cell membrane of tumor cells are excited by electromagnetic radiation, usually in the range of 700nm to 1000nm, releasing energy in the form of heat and inducing cell apoptosis.²⁷ For instance, metal nanoparticles, including nanorods and nanoshells, of materials such as platinum or gold are able to absorb electromagnetic radiation in the infrared region, making them suitable photosensitizers for photothermal therapy.

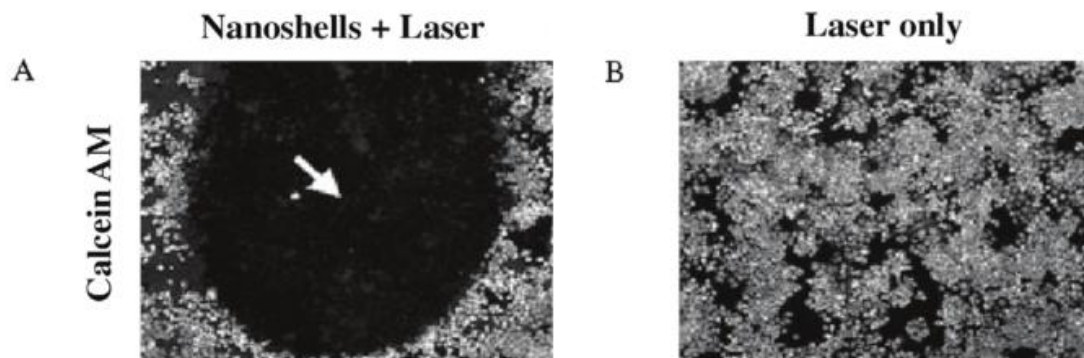


Figure 1.4. (A) Cell samples treated with gold nanoshells and irradiated at 820 nm. The number of cells decreased in the area irradiated by the Laser (less fluorescence signal by Calcein AM). (B) Cell samples only irradiated at 820 nm in the absence of nanoshells. In comparison with Fig 1.4. A, there is a higher number of live cells (higher Calcein AM signal in B).²⁷

2.2. Synthesis of metal nanoparticles. Physico-Chemical and green approaches.

Metal nanoparticles can be synthesized by many physical and chemical approaches, such as using acidic conditions,²⁸ or by precipitation techniques,²⁹ catalytic processes, or decomposition. Although most of these techniques efficiently synthesize metal nanoparticles, they involve several significant drawbacks that limit their application. Regarding environmental aspects, these techniques involve processes at high temperatures and pressures, acidic conditions, and in the presence of toxic chemicals and hazardous wastes. Moreover, these classical processes require an additional functionalization step to increase the biocompatibility of nanoparticles. In fact, despite the benefits and promising potential of nanotechnology for cancer treatment, metal nanoparticles have been found to be cytotoxic to human cells, especially those which have been synthesized by physicochemical methods.³⁰ Therefore, it is necessary to develop new synthesis techniques in accordance with the current environmental and biocompatibility problems.

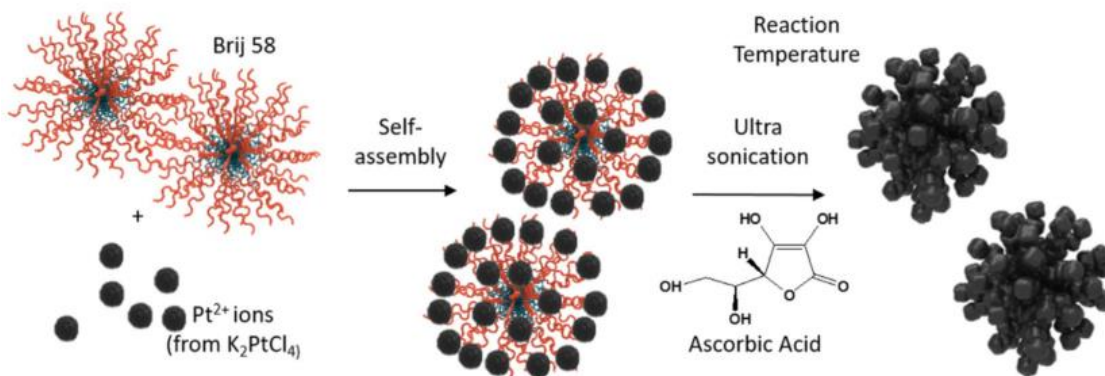


Figure 1.5. Physico-chemical synthesis of platinum nanoparticles in acidic conditions in the presence of surfactants.²⁹

As an encouraging solution for the synthesis of nanoparticles, green chemistry may be able to overcome many of the drawbacks of physico-chemical. The principal aim of the green synthesis is to reduce the generation of hazardous wastes by using water as a solvent, performing syntheses at room temperature and pressure, and avoiding the use of toxic separation agents, generally organic solvents. Collectively, these techniques offer more sustainable and environmentally-friendly processes that can even generate nanoparticles with lower inherent toxicity. This promising group of techniques also includes the use of live organisms, natural products and their bio-compounds as a source of reactive agents.^{31,32} In addition, common plant extracts and food products like coffee or tea (Fig 1.6.), have high sugars, protein, and antioxidant content that make them suitable reducing and capping agents. These natural products can therefore be used to synthesize metal nanoparticles by reducing metal ion salts.³³

Green-synthetic approaches may also be seen as a potential solution for overcoming the cytotoxicity-related limitations of metallic nanoparticles. In many cases, the cytotoxicity of green synthesized nanoparticles is a result of coatings that surrounds the metal nanoparticles. These coatings are integrated onto the nanoparticle surface by

organically-derived compounds presents in the media that are attached to the metal nanoparticle surface. However, despite the advantages, nanoparticles synthesized by green methods often produce ununiform reaction products with varying sizes and shapes.³⁴

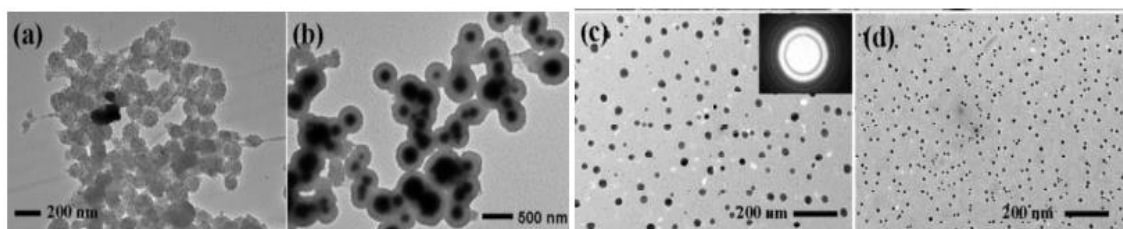


Figure 1.6. Characterization of green synthesized nanoparticles by TEM. Gold nanoparticles were synthesized using coffee extract in aqueous solution.³³

The synthesis of metal nanoparticles using natural products, such as coffee and tea is not the only possible green route of nanoparticle synthesis. Living organisms such as bacteria can also synthesize metal nanoparticles in the appropriate conditions.³⁵ The two principal routes of cell-based nanoparticle synthesis are extracellular and intracellular, and are dependent on a type of bacteria. *Pseudomonas stutzeri* AG259, a bacteria presented in silver mines, has been reported to reduce silver metal ion salts to form silver nanoparticles.³⁶

The synthesis mechanisms, antimicrobial properties, and anticancer properties of green synthesized nanoparticles, mainly using natural products, has been successfully studied.³⁷ However, the synthesis of metallic nanoparticles through the use of living organisms, particularly of human cells, is still poorly understood. Furthermore, few studies have reported the synthesis of metal nanoparticles using different classes of human cells;^{38,39} additionally, there is still a lack of information regarding the mechanism of cell-based

syntheses. Lastly, to our knowledge, the cytotoxicity of nanoparticles synthesized by human cells has not been tested *in vitro* and *in vivo*.

2.3. Interactions between metal nanoparticles and cancer cells.

Some transition metals, metals which have partially filled d orbitals such as gold, iron, or copper, are important for cellular metabolism and are therefore essential for cell life.⁴⁰ Studies of the interaction between these metals and cells are vital to understand the differential cell responses in the presence of various metals and cell types.

When metal nanoparticles cross the cell membrane, they interact with proteins, enzymes, and organelles, which ultimately aim to degrade the nanoparticle. This process produces a series of metal ions and, more important, reactive oxygen species (ROS).⁴¹ ROS are reactive oxygen compounds such as peroxides, superoxides, singlet oxygen, etc. Normally, they are naturally formed as by-products during oxygen metabolism but are easily stabilized; however, the presence of metal nanoparticles excessively increases this formation and creates stress within the cell⁴²

When the level of ROS increases inside cells, serious damages to amino-acids in proteins and enzymes and nucleotides in DNA occur, inducing stress to the cells. Most important is the damage caused by ROS to the cell mitochondria. This damage occurs because of oxidizing NADH into NAD⁺. Because NADH is involved in ATP production, the energy source of the cell, oxidation of this molecule impairs energy production and subsequently induces the cellular apoptosis (Fig 1).⁴³ Additionally, irradiation of cancer cells that have been targeted with metal nanoparticles can further increase the level of ROS production.⁴⁴ In fact, green-nanoparticles can trigger cancer

cell apoptosis using the same mechanism that promotes their antimicrobial response: generation of ROS and release of metal ions. However, when compared to physico-chemically produced nanoparticles, green synthesized metal nanoparticles have a lower cytotoxicity towards healthy cells that reduces ROS formation.⁴⁵

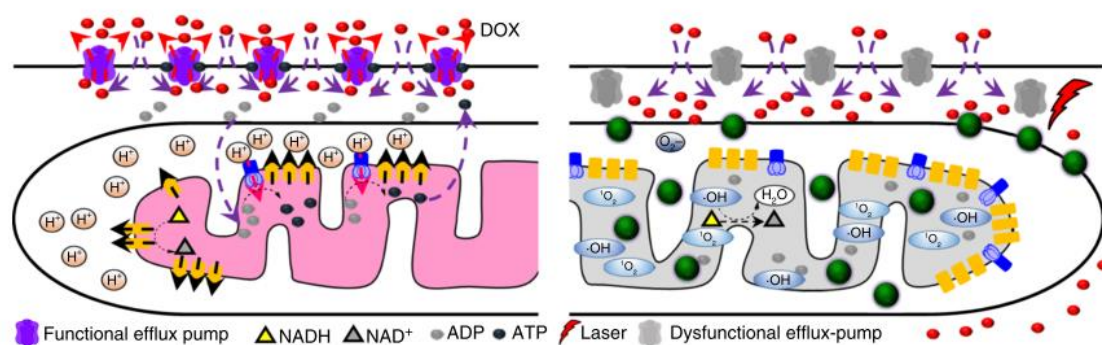


Figure 1.7. Comparison between the standard activity of ATP production in mitochondria (left) and the generation of ROS through a combination of irradiation and metal nanoparticle targeting (right).⁴³

3. State of the art

3.1. Synthesis of metal nanoparticles using human cells

As was previously mentioned, the synthesis of metal nanoparticles using human cells has not been deeply studied. However, several groups have successfully used this method to generate green-nanoparticles. For example, Venkataraman and collaborators were able to synthesize gold nanoparticles using human cells (cancerous and non-cancerous cells) in place of, previously reported bacteria cells. By adding a solution of HAuCl_4 to cell media, cells were observed to reduce these metal ions into nanoparticles. These nanoparticles were found both attached to the cell membrane and distributed throughout the cytoplasm. Although the mechanism of nanoparticle synthesis in human cells has not yet been determined, Venkataraman *et al* proposed that the nanoparticles were the cell's inherent metabolism.³⁸ El-Said and collaborators obtained similar results in the synthesis of gold nanoparticles when, using the same cell lines. Consistent with other methods used for green-nanoparticle synthesis, the nanoparticles obtained in this study were of different sizes and shapes.³⁹ Despite these studies, there are currently no have investigated the cytotoxicity of these nanoparticles. Moreover, the only known studies involving the green synthesis of nanoparticles with human cells have synthesized gold nanoparticles. To the best of our knowledge, no other metal or metal has been tested.

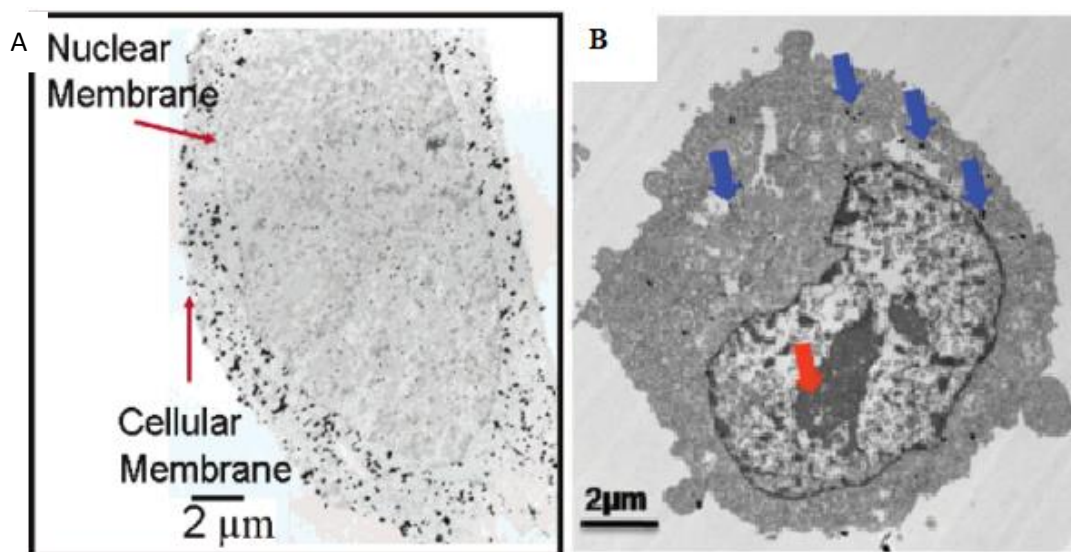


Figure 2.2. (A) TEM image of HEK 293 cells with gold nanoparticles (Black spots) within the cytoplasm³⁸ (B) TEM image of MCF-7 cells with similar characteristics. Blue and red arrows denote the location of gold nanoparticles throughout the cytoplasm.³⁹

3.2. Applications of metal nanoparticles in cancer treatments.

Nanoparticles meet the essential cancer therapeutic requirements of efficacy and selective toxicity. One of the most promising nanomaterials for cancer treatments is gold nanoparticles, since they are highly stable, sensitive, and can be manufactured using a variety of techniques with high precision. For instance, gold nanoparticles have been synthesized through the reduction of ion gold salts with sodium citrate as a reducing and stabilizing agent in boiling water.⁴⁶ They have also been synthesized by different green approaches using natural sources like antioxidant extracts from blackberries, blueberries and pomegranate.⁴⁷ For example, Kajani and collaborators previously synthesized gold nanoparticles using *Taxus baccata* extracts in aqueous and ethanolic solutions. Through *in vitro* studies with different cancer and non-cancer cell lines, they found that the nanoparticles impacted cell morphology, and, as expected, cell viability.⁴⁸

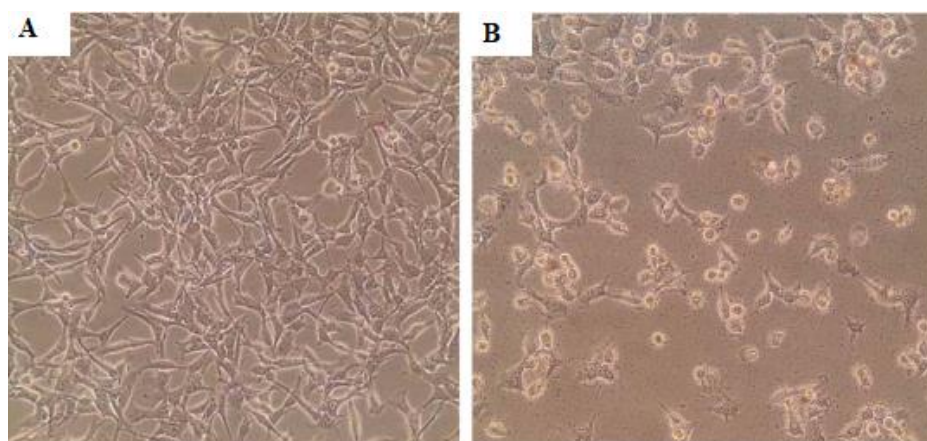


Figure 2.1. Changes in the morphology of MCF-7 cancer cells after treatment with gold nanoparticles synthesized using *Taxus baccata extract*.⁴⁸

Additionally, platinum nanoparticles have also been reported to have significant anticancer activity, especially when synthesized by a green method. Apart from the synthesis of platinum nanoparticles by green methods, physico-chemical approaches of these nanoparticles have also been reported as potentially promising anticancer drugs. For example, Teow and collaborators synthesized platinum nanoparticles by reducing platinum acid with NaBH_4 , which were then capped with folic acid to increase the biocompatibility. The obtained nanoparticles showed high anticancer activity in multiple cancerous cell lines even at low concentrations; however, this two steps synthesis requires more additional time when compared with green synthesis; where nanoparticle capping is inherently produced during nanoparticles synthesis.⁴⁹

Similar to gold, platinum and palladium nanoparticles, the synthesis and anticancer properties of bimetallic nanoparticles have also been deeply studied. Tea polyphenols (TPP in figure 2.3) have been used as reducing and stabilizing agents for the synthesis of Au-Pt bimetallic nanoparticles. These nanoparticles were found to induce apoptosis and inhibit proliferation in different human cervical cancer cells.⁵⁰ Additionally, bovine serum

albumin (BSA) and gold-silver nanoclusters have been prepared as DNA carriers by Dutta and collaborators. These nanoaggregates were found to be a promising technique for gene delivery in cancer theranostics, due to the cytotoxicity of Au-Ag bimetallic nanoparticles and the therapeutic activity of the gene delivery.⁵¹

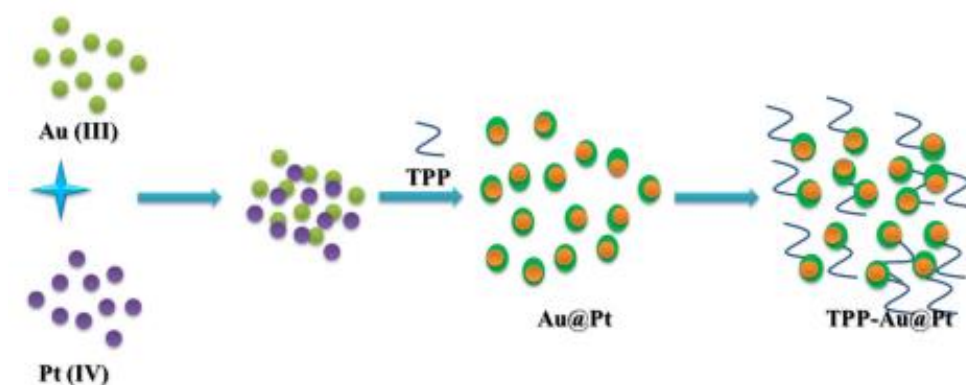


Figure 3.3. Scheme of synthesis for Au-Pt bimetallic nanoparticles using tea polyphenols as reducing and stabilizing agents.⁵⁰

3.3. Applications of metal nanoparticles in photothermal treatments.

Photothermal treatment, when combined with metal nanoparticles is a promising technique for many cancer types. However, its potential for the treatment of glioblastoma is especially impressive. To date, several types of nanoparticles, especially magnetic nanoparticles, have been tested in patients using thermotherapy, where magnetic nanoparticles are heated through exposure to a magnetic field with the end goal of killing tumor cells.⁵¹ However, the use of nanoparticles in photothermal therapy is still being tested due to aspects regarding cytotoxicity.

Currently, gold nanorods have been one of the most promising nanoparticles for photothermal treatments, since they have a strong absorption in the near infrared (NIR) range. When conjugated with specific antibodies, gold nanorods can target and kill cancer cells when exposed to NIR irradiation.⁵² On the other hand, Tang and collaborators synthesized 4 nm palladium nanosheets coated with glutathione with a strong absorption in the NIR. These nanosheets were tested *in vivo* for photothermal therapy in kidney tumors, showing high accumulation of nanosheets in the tumor and complete tumor ablation.⁵³ when irradiated with a NIR laser

In addition, gold over branched palladium nanostructures of 100 nm were developed by McGrath and collaborators, where gold nanoparticles grew over a multibranch nanostructure of palladium. This nanostructure yielded a broad absorption band in the near infrared range, making it very suitable for use in photothermal therapy. In fact, *in vivo* photothermal studies using these nanostructures showed a high decrease in HeLa tumor size.⁵⁴

The anticancer properties of platinum nanoparticles have also recently been studied for their application in photothermal therapies. Alshatwi and collaborators developed a route of synthesis using a tea extract based on polyphenols. These platinum nanoparticles showed high anticancer activity in human cervical cells, inducing apoptosis and inhibiting cell proliferation when exposed to photothermal radiation.⁵⁵

4. Materials and Methods

4.1. Materials.

Glioblastoma cells and Eagle's Minimum Essential Medium (EMEM) were purchased from ATCC; Fetal Serum Bovine (FBS), Phosphate Buffered Saline (PBS), penicillin, and LIVE/DEAD™ Viability/Cytotoxicity Kit for mammalian cells were purchased from Thermo Fisher. MST assay was purchased from Promega. K_2PtCl_4 , K_2PdCl_4 , $HAuCl_4$, methanol and 2,7-dichlorofluorescein diacetate were purchased from Sigma-Aldrich. The rest of the materials such as well plates, culture flasks, centrifuge tubes and scrapers were purchased from Falcon. 300 mesh copper-coated carbon grids were purchased from Electron microscopy science, hatfield, PA.

4.2. Synthesis of G-Au/Pt and G-Au/Pd nanoparticles.

Cell Incubation: Glioblastoma cells were grown in EMEM supplemented with 10% Fetal Bovine Serum (FBS) and 5% penicillin and incubated at 37 °C with 5% of CO₂ until the cultures reached 90% of confluency. Next, the growth medium was removed and the cells were washed twice with phosphate buffered saline (PBS), followed by the addition of 10 ml of 10⁻³ M $HAuCl_4$ and K_2PtCl_4 for G-Au/Pt nanoparticles and 10 ml of 10⁻³ M $HAuCl_4$ and K_2PdCl_4 for G-Au/Pd nanoparticles in absence of EMEM. The culture flasks were incubated for 4 days and observed using a phase contrast microscopy before adding metallic salts and adding them at 0 hours, 24 hours and 96 hours.

Cell lysis and nanoparticle extraction: After 96 hours, cells were scraped from the media and transferred into centrifuge tubes, sonicated for 1 hour and centrifuged at 11000 rpm and 4 °C for 30 minutes. Then, the supernatant was removed, and the pellet was resuspended in deionized water. This procedure of sonication-centrifuge and resuspension was repeated twice. Finally, the bimetallic nanoparticles were obtained by freezing at -80 °C and lyophilizing for 1 day.

4.3. Synthesis of G-Au/Pt-Tr and G-Au/Pd-Tr nanoparticles

Cell incubation and cell lysis for nanoparticle synthesis were carried out as previously described. However, to generate G-Au/Pt-Tr and G-Au/Pd-Tr nanoparticles, after the second cycle of sonication-centrifuge pellets were resuspended in ethanol and stirred for 16 hours at 500 rpm. The resulting suspension was sonicated for 20 minutes and centrifuged at 10000 rpm and 25 °C for 20 minutes. Similarly, nanoparticles were obtained by freezing at -80 °C and lyophilizing for one day.

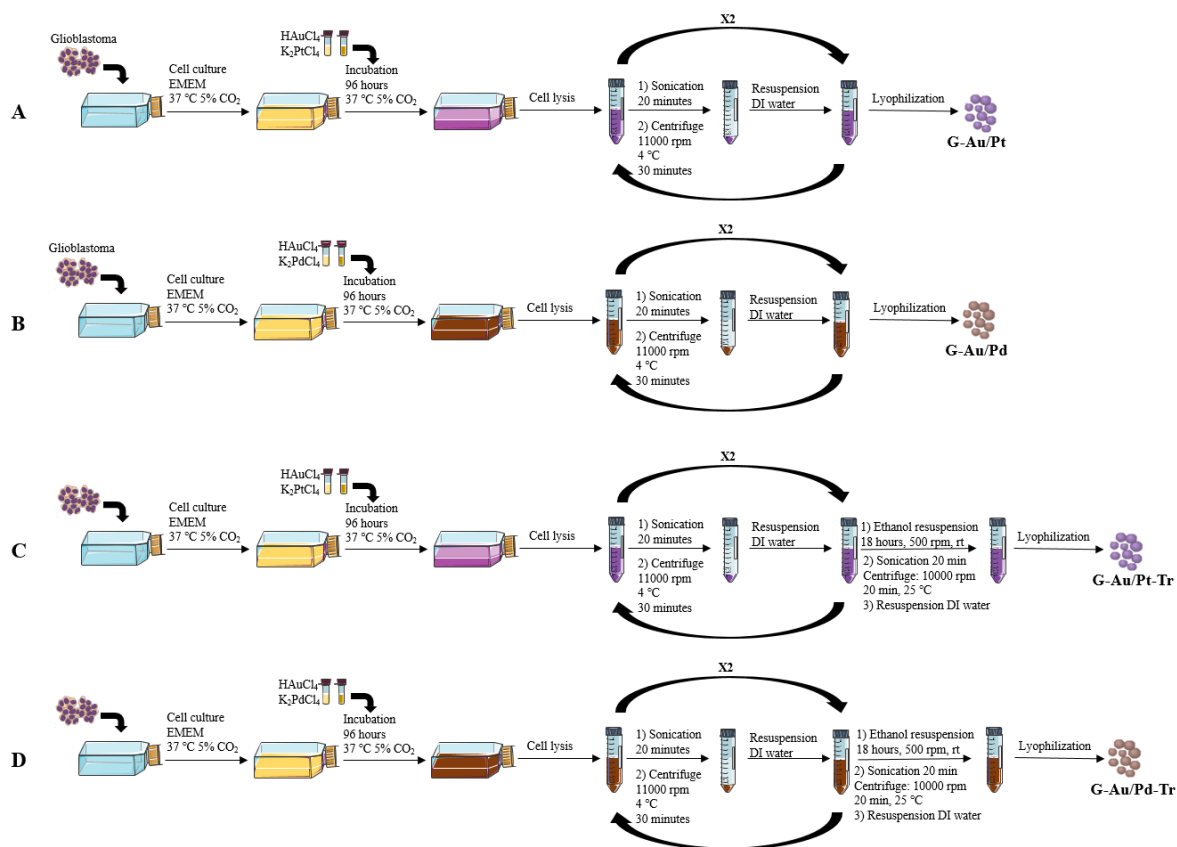


Figure 4.1. Scheme of synthesis for (A) G-Au//Pt (B) G-Au/Pd, (C) G-Au/Pt-Tr and (D) G-Au/Pd-Tr.

4.4. Transmission Electron Microscopy

The nanoparticles obtained before and after ethanol treatment were suspended in deionized water and placed on 300 mesh copper-coated carbon grids. These samples were analyzed using a JEM-1010 Transmission Electron Microscope (JEOL USA Inc., MA) at 80 kV.

4.5. Energy-dispersive X-Ray Spectroscopy analysis (EDS)

The obtained nanoparticles before ethanol treatment were suspended in deionized water and placed on 300 mesh copper-coated carbon grids. Then, they were analyzed with a Scanning Electron Microscope (SEM, HitachiS-4800) equipped with Energy Dispersive X-ray analysis (EDS).

4.6. UV-Vis Spectrophotometry Analysis

Glioblastoma cells were seeded in an additional 6 well plate and incubated in EMEM at 37 °C and 5% CO₂ for 24 hours. Cells were then rinsed with PBS, followed by the addition of 1.5 ml of a solution of 10⁻³ M HAuCl₄ and K₂PtCl₄ for G-Au/Pt nanoparticles and 1.5 ml of 10⁻³ M HAuCl₄ and K₂PdCl₄ for G-Au/Pd nanoparticles. The 6 well plate was then incubated for 4 days and UV-Vis spectra were recorded every 24 hours, up to 96 hours, and after cell lysis.

4.7. Cytotoxicity assays.

The anticancer activity of G-Au/Pt, G-Au/Pd, G-Au/Pt-Tr and G-Au/Pd-Tr in glioblastoma cells and human dermal fibroblasts (HDFs) was determined by MTS assays (3-(4,5-dimethylthiazol-2-yl)-5-(3-carboxymethoxyphenyl)-2-(4-sulfophenyl)-2H-tetrazolium). For this, cells were seeded in 96 well plates at a density of 5x10⁴ cells per mL and cultured for 24 hours at 37 °C with 5% CO₂. EMEM was used to culture glioblastoma cells, whereas Dulbecco's Modified Eagle Medium (DMEM) was used for HDFs. After 24 hours, media was replaced and nanoparticles were added at different

concentrations (5, 10, 15, 25, 50, 75 and 100 $\mu\text{g mL}^{-1}$) and incubated for 24, 72 and 120 hours. The medium was then discarded and 100 μL of MTS (1:5 diluted in the corresponding media) was added to each well and incubated at 37 °C for 3 hours. The absorbance of each well plate was measured using EspectraMax M3 spectrophotometer (Molecular Devices, Sunnyvale, CA) at 490 nm.

4.8. Determination of Reactive Oxygen Species.

The intracellular production of ROS was determined using 2,7-dichlorofluorescein diacetate (DCFH-DA), which passively enters cells and reacts with ROS producing dichlorofluorescein (DCF), a fluorescent compound. Glioblastoma cells were seeded in a 24 well plates at a density of 5×10^4 cells per mL and cultured in EMEM for 24 hours at 37 °C with 5% CO_2 . After 24 hours, media was removed and nanoparticles (G-Au/Pt and G-Au/Pd) were diluted in media at 20 $\mu\text{g mL}^{-1}$ and added to cells, which were then incubated at 37 °C for 24 hours. The media was subsequently removed and wells were washed twice with PBS. A 10 mM stock solution of 2,7-dichlorofluorescein diacetate (DCFH-DA) in methanol was diluted in PBS to yield a 100 μM concentration and added to each well and incubated at 37 °C for 30 minutes. Fluorescence of well plate was measured at 485 nm excitation and 520 nm emission using EspectraMax M3 spectrophotometer.

4.9. Photothermal Treatment.

Glioblastoma cells were cultured in EMEM and seeded in 96 and 12 well plates and incubated at 37 °C and 5% CO₂ for 24 hours. Then, cells were incubated at different concentrations of G-Au/Pt nanoparticles (5-100 μg mL⁻¹ for 96 well plates and 15-50 μg mL⁻¹). The well plates were irradiated by a 785-nanosecond diode laser at a power of 1W for 10 and 15 minutes. After irradiation, the 96 well plates were examined by MTS assay to evaluate cell viability following the same procedure as described in cytotoxicity assays. The 12 well plates were rinsed with PBS and the cells were stained using a Viability/Cytotoxicity kit for mammalian cells. This kit used Calcein AM to label live cells and Ethidium homodimer-1 to label dead cells. After incubating at room conditions, the well plates were observed under a ZEISS Axio Observer Z1 fluorescence microscopy (Zeiss, Oberkochen, Germany) under a 20x objective lens.

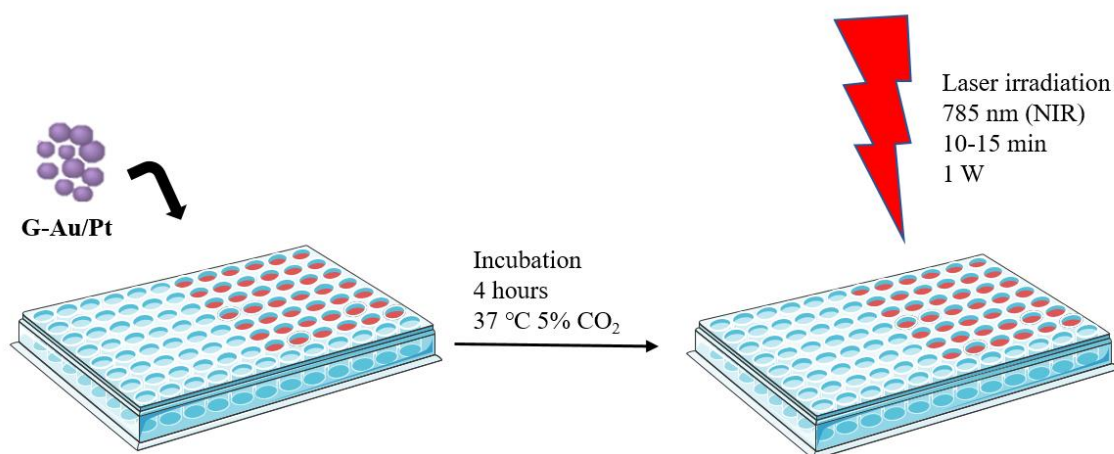


Figure 4.2. *In vitro* Photothermal Therapy of glioblastoma cells by using G-Au/Pt nanoparticles and irradiating at 785 nm.

5. Results and discussion

5.1. Synthesis of bimetallic nanoparticles

The reaction process was monitored by phase contrast microscopy at the beginning and end of experiments (Fig. 5.1). At 0 hours (addition of metallic ion salts), the glioblastoma cells begin to die due to the absence of nutrients and the high concentration of metallic ions. This was corroborated by the increase in brightness around the cell peripheries, which was caused by their detachment from the well culture flask.

At 24 hours, nearly all cells were death, and those that remained attached had an altered colour but kept their original morphology. These changes were likely caused by the bio-reduction of gold, platinum and palladium in their corresponding culture flasks. In G-Au/Pt culture flasks (Fig. 5.1.A), the inner part of cells similarly turned a darker colour, whereas cells in the G-Au/Pd culture flasks (Fig. 5.1.B) turned into gold colour, indicative of the formation of nanostructures.

At 96 hours, no significant changes in colour and morphology were observed when compared to 24 hours after metallic salt addition. This finding suggests that product of reaction formed during the first 24 hours of incubation. Until 96 hours, the dispersion of colour around the cell surface, especially in G-Au/Pt cells suggests that the synthesized products may be partially released from cells to the media.

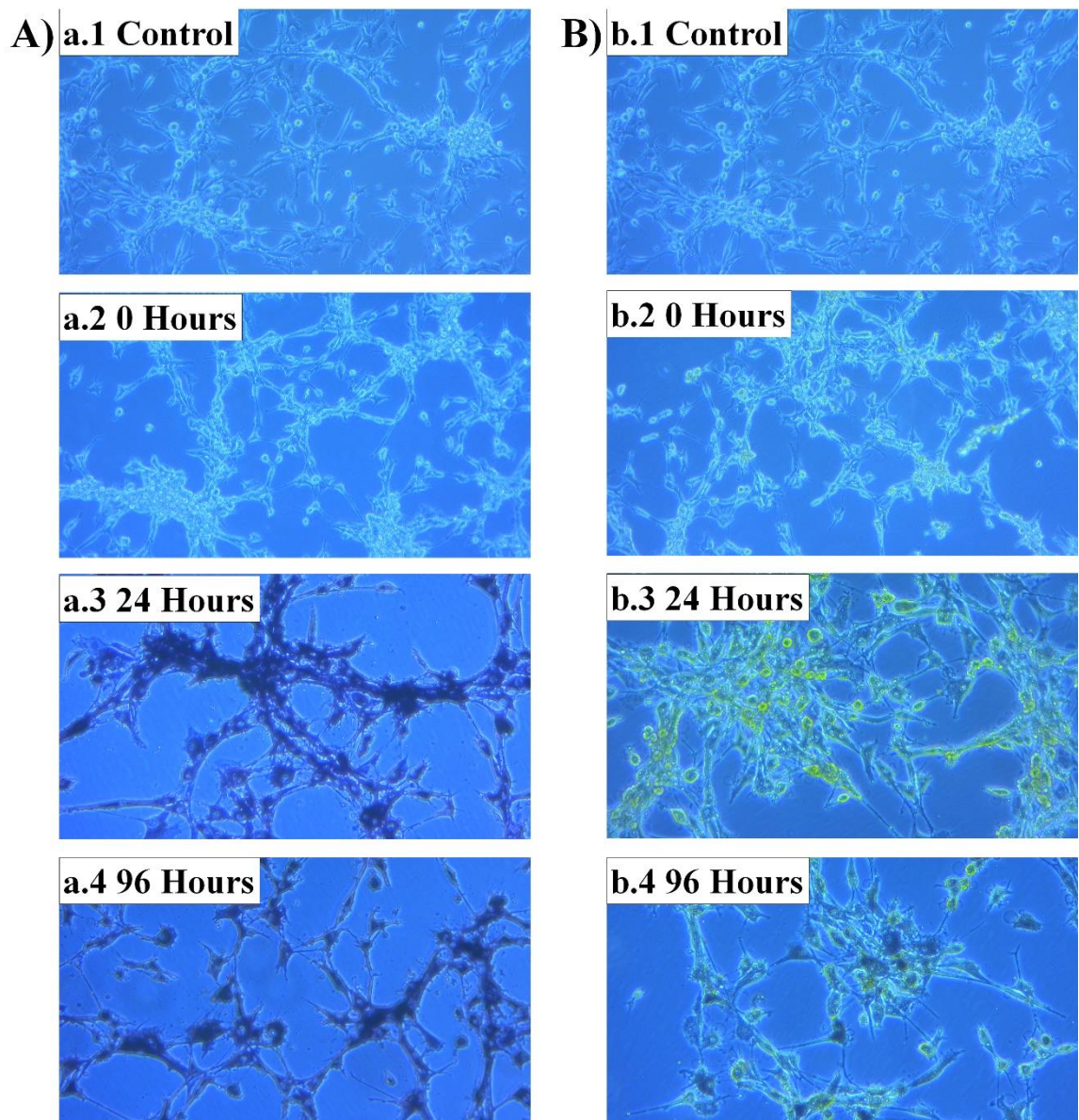


Figure 5.1. Phase contrast microscopy images of the synthesis of (A) G-Au/Pt and (B) G-Au/Pd. Pictures were taken before the addition of metallic salts (a/b.1), directly after the addition of metallic ion salts (a/b.2) 24 hours of reaction (a/b.3) and 96 hours of reaction (a/b.4).

During phase contrast experiments, the synthesis of nanoparticles was simultaneously monitored by periodic measurements of absorbance using 6 well plates containing glioblastoma cells and metallic salts.

The synthesis of G-Au/Pt nanoparticles was evidenced an increase in absorbance at 555 nm after the 24 hours of incubation (Fig. 5.2 B). The subsequent measurements demonstrated the end of nanoparticle synthesis as shown by a slight decrease in absorbance. This phenomenon may be a result of the aggregation of nanoparticles or due to the deposition of nanoparticles to the bottom of wells. To determine whether nanoparticles were still encapsulated within cells, cells were lysed after 96 hours of reaction and the absorbance was again measured. We found a significant increase in absorbance, which we hypothesize was caused by the release of bimetallic nanoparticles from inside the cells. This increase in absorbance corroborates finding that the majority of nanoparticles is synthesized by an intracellular mechanism, as was previously reported by Venkataraman and collaborators.³⁸ Additionally, this supports our phase contrast results in which intracellular space produced a darker colour than the surrounding solution (Fig. 5.1.)

Moreover, the range of observed absorption was similar to the surface plasmon resonance band of gold nanoparticles, since platinum doesn't present any absorption in this range.

To determine the synthesis of G-Au/Pd nanoparticles, UV/Vis absorption spectra were similarly (Figure 5.2 C). In comparison to the spectra obtained for G-Au/Pt nanoparticles, we observed limited changes in the absorbance for G-Au/Pd nanoparticles. Even after cell lysis at 96 hours of incubation, no increase in absorbance was observed.

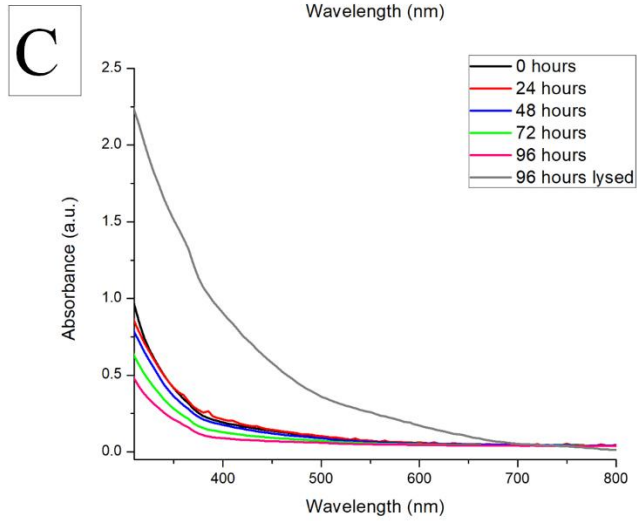
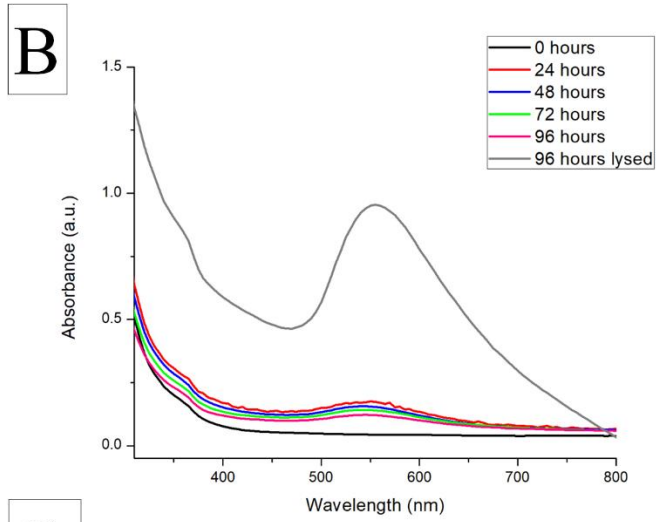
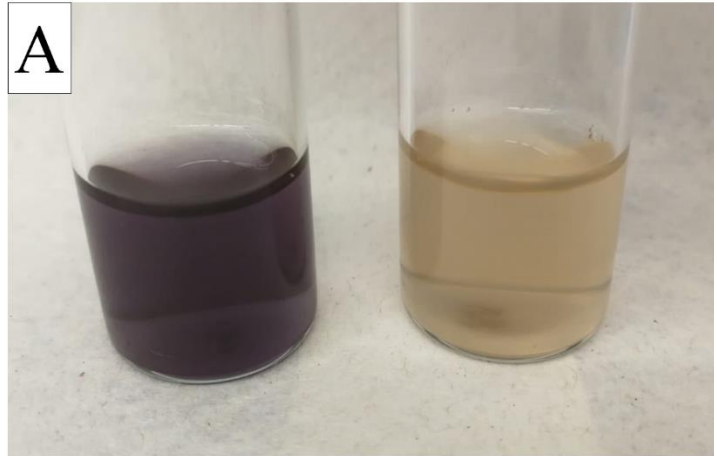


Figure 5.2. (A) G-Au/Pt (left) and G-Au/Pd (right) solutions suspended in water. Reaction monitoring by UV-Visible absorption spectra for the synthesis of (B) G-Au/Pt nanoparticles and (C) G-Au/Pd nanoparticles by glioblastoma cells.

Elemental analysis by Energy-Dispersive X-Ray Spectroscopy (EDS) was performed to further determine whether nanoparticle synthesis was successful (Fig. 5.3). These experiments corroborated the presence of the main compounds used in the synthesis for each nanoparticle: gold and platinum for G-Au/Pt (Fig 5.3 A) and gold and palladium for G-Au/Pd (Fig 5.3 B). This is evidenced by peaks at Moreover, the presence of additional elements apart from the metals can be observed in both synthesized nanoparticles. Species such as oxygen and carbon corroborate the presence of organic compounds in the sample, which is expected due to the green synthesis procedure in both types of nanoparticles. In addition, species such as potassium and chloride are present in the initial reagents, which are likely derived from the initial reagents that remained in the samples after purification. Lastly, species such as sodium may represent impurities in the sample and may originate from PBS used during synthesis.

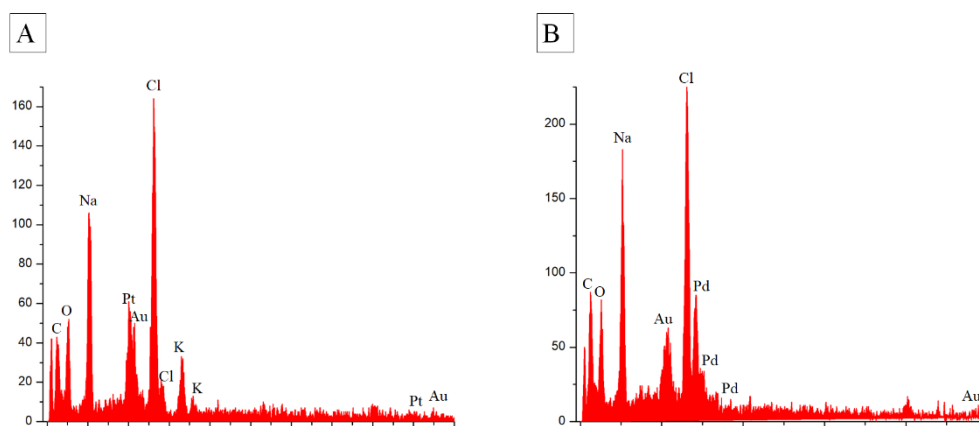


Figure 5.3. EDS spectra representing elemental analysis of (A) G-Au/Pt and (B) G-Au/Pd nanoparticles.

To evaluate the formation of bimetallic nanoparticles, the species G-Au/Pt and G-Au/Pd (Fig 5.4 C and D) were examined by transmission electron microscopy (TEM) and both showed an average size of 21.2 ± 7 nm. Although the size of metal nanoparticles in both species is similar, the shape varies from nanoparticle to nanoparticle. In case of G-Au/Pt (Fig 5.4 A and B), the majority are spheres with irregular sides, though other geometric structures with regular sides are observed. However, in case of G-Au/Pd (Fig 5.4 C and D), a higher content of cubes, pyramid or rhombic structures than in G-Au/Pt is observed, although the predominant shape is still the sphere. Additionally, the species G-Au/Pt and G-Au/Pd were observed to have been partially released from the cellular matrix, as most of the metal nanoparticles are surrounded by this material and formed bigger aggregates.

Both species of nanoparticles were treated by suspension and stirring in ethanol for 16 hours, to remove cellular material that yielded G-Au/Pt-Tr and G-Au/Pd-Tr. These second species, shown in Fig 5.4 (E, F, G and H), appear to have important differences from each other. In the case of G-Au/Pt-Tr, the treatment with ethanol appears to be insufficient, as there was a large amount of cell material remaining in the sample, which may obstruct the release of nanoparticles. In case of Au/Pd-Tr, apart from remaining in the cellular matrix, the metallic nanoparticles are smaller than before the ethanol treatment, with a size of $9,7 \pm 4$ nm. The TEM results confirm that the ethanol treatment is not the best solution to disaggregate the metal nanoparticles from cellular material, so new techniques of purification should be applied to fulfil this purpose.

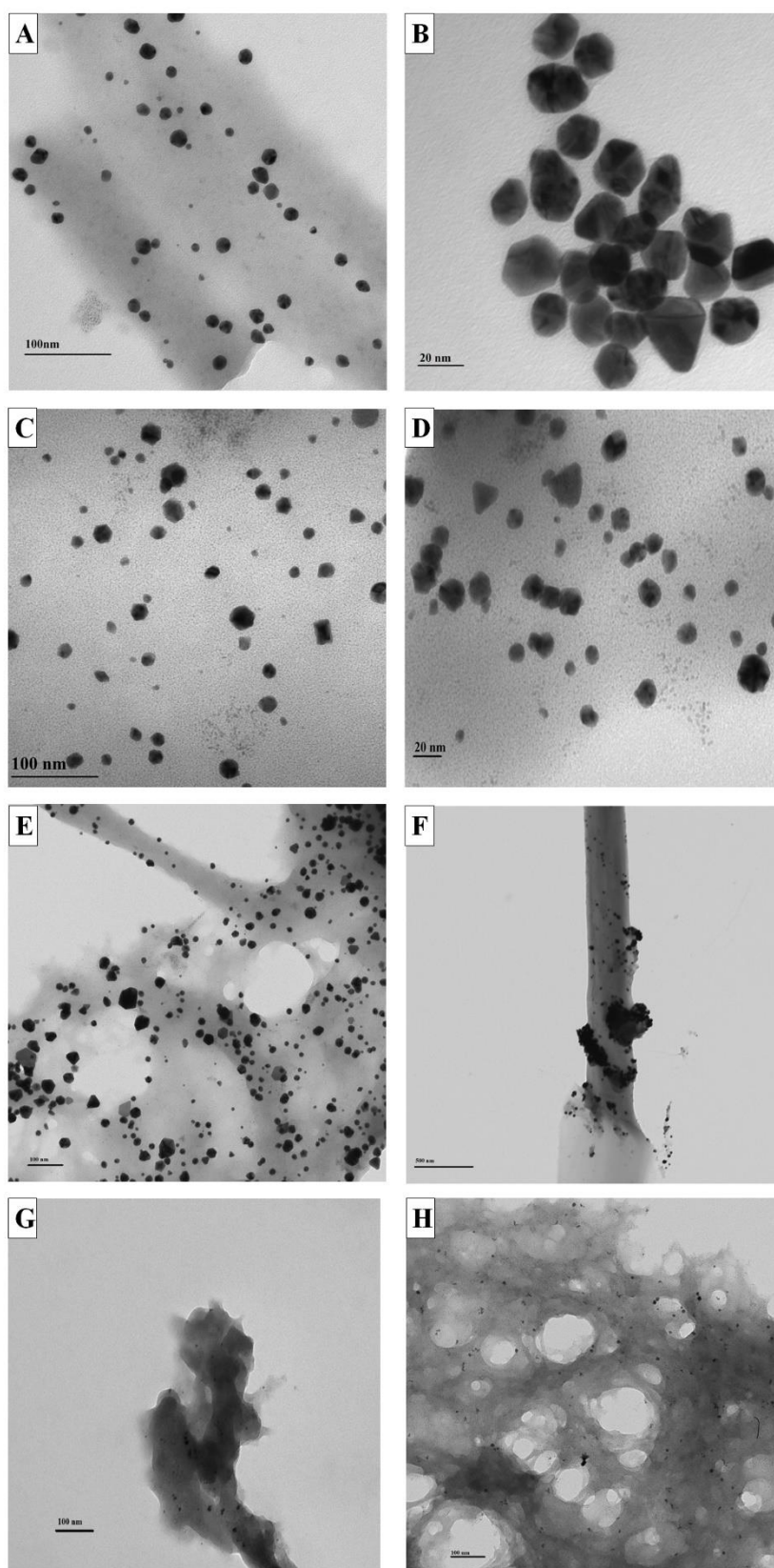


Figure 5.4. TEM images for evaluating the size and shape of nanoparticles and the success of ethanol treatment for the species G-Au/Pt (A, B), G-Au/Pd (C, D), G-Au/Pt-Tr (E, F) and G-Au/Pd-Tr (G, H).

5.2. Cytotoxicity studies in Human Dermal Fibroblasts and Glioblastoma cells.

To evaluate the anticancer activity in glioblastoma cells and the biocompatibility in HDF of two synthesized metal nanoparticles, before and after the ethanol treatment, the cells were incubated in the presence of these species at different concentrations for periods of one, three and five days.

Synthesized G-Au/Pt nanoparticles (Fig 5.5 A) were observed to have anticancer properties in glioblastoma cells within the first day of incubation, showing a significant decrease in cell viability in all concentrations compared to the control, with a maximum decrease of 40% at $15 \mu\text{g mL}^{-1}$. After the ethanol treatment of G-Au/Pt, the anticancer activity of G-Au/Pt-Tr observed at 24 h of incubation is not improved at any concentration range.

After the first day of incubation, glioblastoma cells consumed all the nanoparticles that were present in the media, or at least those that were released from the cellular matrix. This hypothesis is validated by the cell proliferation observed at all the nanoparticle concentrations, with no significant differences compared to the control in both, treated and untreated G-Au/Pt nanoparticle. Also, the biocompatibility of G-Au/Pt and G-Au/Pt-Tr was studied in HDF cells (Fig. 5.5 B) at the same concentrations and during the same periods of incubations. In all the cases, both treated and untreated species show an increase in cell proliferation with noticeable differences from the control, except for the incubation of G-Au/Pt-Tr during the first 24 h, where a decrease of cell viability of HDF is observed at high concentrations. This increase in cell viability along the time suggest that these nanoparticles enhance the cell growth in healthy species.

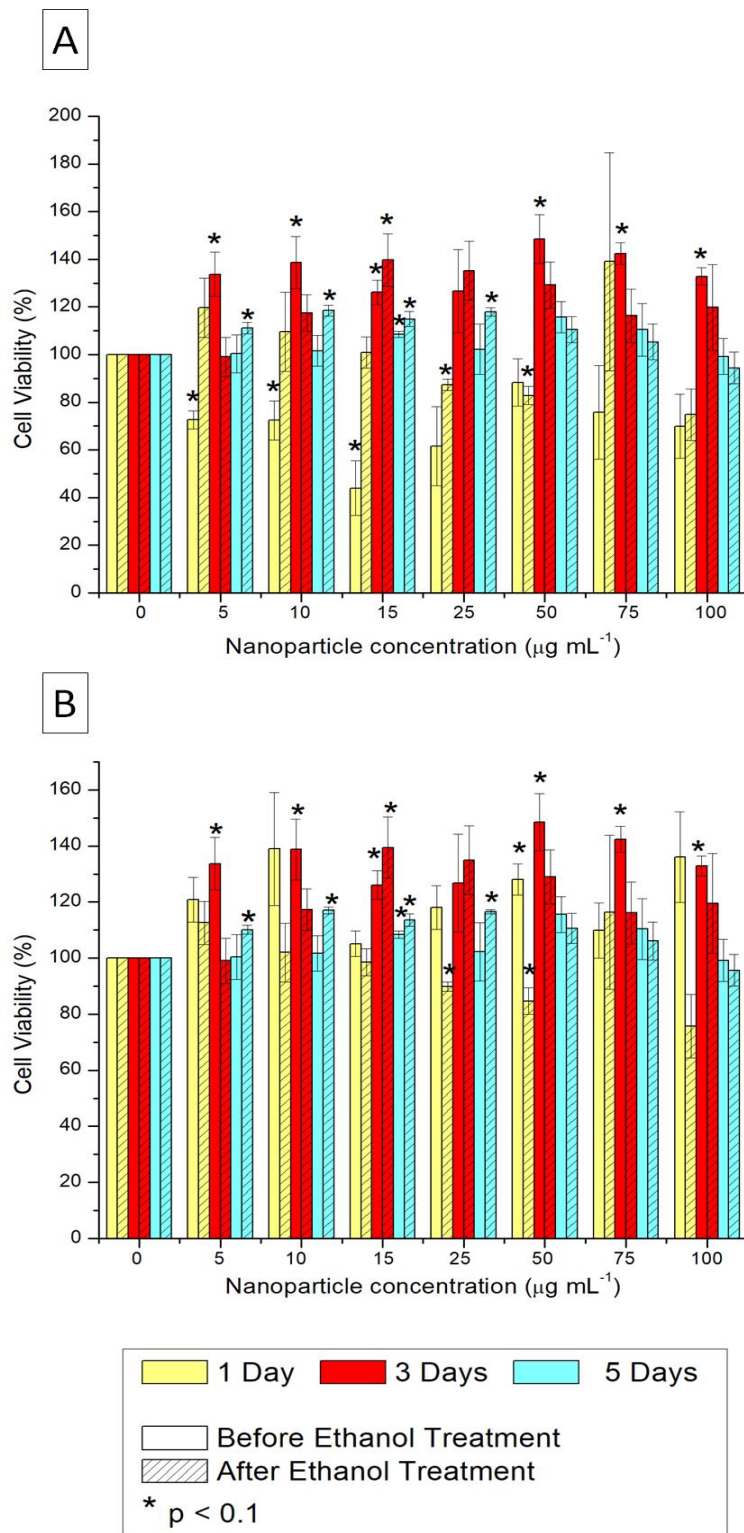


Figure 5.5. Viability percentage of Glioblastoma (A) and Human Dermal Fibroblasts (B) at different concentrations of G-Au/Pt and G-Au/Pt-Tr incubated during 1, 3 and 5 days.

Additionally, synthesized G-Au/Pd nanoparticles (Fig 5.6.) did not exhibit any anticancer activity at any concentration, except at $15 \mu\text{g mL}^{-1}$ with significant differences and a 40% decrease in the cell viability. G-Au/Pd-Tr also do not show any significant anticancer properties, similar to G-Au/Pt-Tr nanoparticles. This observation suggest that the ethanol treatment is ineffective for the enhancement of anticancer properties and for the release of metal nanoparticles from the cellular matrix.

Upon the analysis of biocompatibility for the G-Au/Pd nanoparticles, the cell viability slightly decreases during the first 24 hours of incubation, however, after this period, the cells began to grow constantly with no significant differences compared to the control, and at certain concentrations (5 and $10 \mu\text{g mL}^{-1}$ at 5 days) they show an increase in the cell proliferation.

Although G-Au/Pd nanoparticles do not present anticancer properties when compared to G-Au/Pt nanoparticles, their biocompatibility could afford their use in other applications, such as imaging, or even drug carriers.²⁶

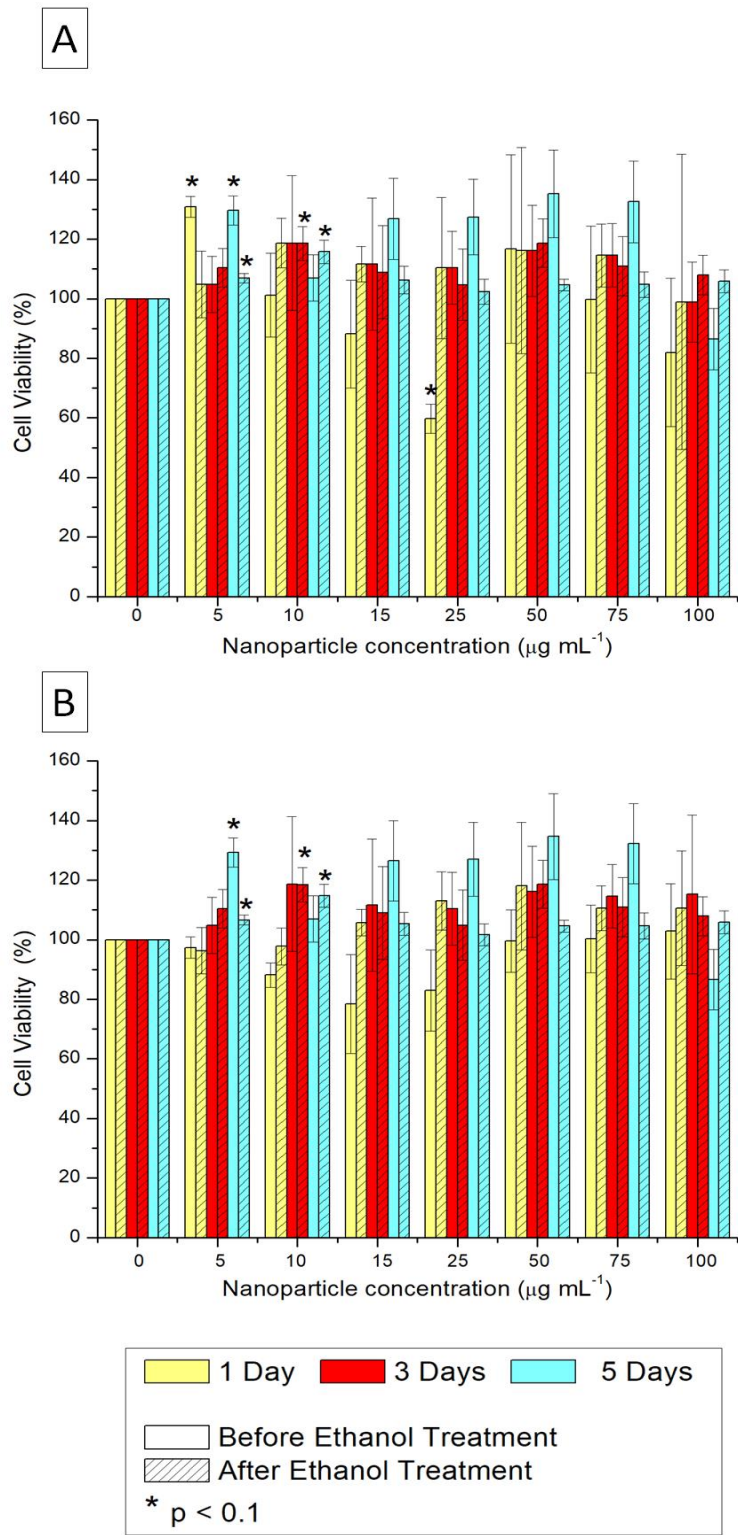


Figure 5.5. Viability percentage of Glioblastoma (A) and Human Dermal Fibroblasts (B) at different concentrations of G-Au/Pd and G-Au/Pd-Tr incubated during 1, 3 and 5 days.

5.3. Intracellular measure of reactive oxygen species

Reactive Oxygen Species (ROS) were measured after incubation with G-Au/Pt and G-Au/Pd for 24 h at $20 \mu\text{g mL}^{-1}$, a suitable concentration that shows a high anticancer activity since it was observed in the cytotoxicity studies (Fig. 5.6).

The cells incubated with G-Au/Pt displayed an increase of 40% in the production of ROS after 24 h, although it is a low value if compared to an increase of 400% in ROS generation for ZnO nanoparticles at the same concentration.⁴¹ On the other hand, G-Au/Pd did not show any significant generation of ROS, reporting a similar value to the control. These results agree with the cytotoxicity studies and anticancer properties in glioblastoma cells. G-Au/Pt can penetrate through the cell membrane and produce stress into the cell by the generation of ROS; however, G-Au/Pd nanoparticles may be not allowed to cross the cell membrane and create this stress that leads to the cell death.

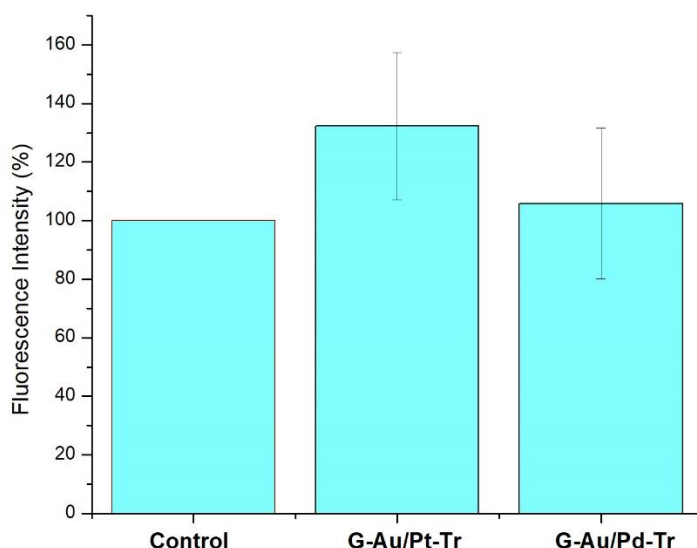


Figure 5.6. Reactive Oxygen Species (ROS) generation by glioblastoma cells incubated with G-Au/Pt and G-Au/Pd nanoparticles for 24 hours.

5.4. Photothermal therapy of Glioblastoma cells using G-Au/Pt nanoparticles.

Glioblastoma cells were incubated with G-Au/Pt nanoparticles at different concentrations for 4 h and then irradiated at 785 nm for 15 min and stained with Calcein AM and Ethidium Homodimer-1. To qualitatively evaluate the efficacy of this treatment, the treated cells, observed under fluorescence microscopy (Fig. 5.7) showed a loss of Calcein AM signal (green) and an increase in Ethidium Homodimer-1 signal (red) compared to the control.

This appearance of the red signal upon excitation at 785 nm indicates cell death that may be caused by the addition of G-Au/Pt and irradiation at 785 nm. The increase in expression of red fluorescence produced by dead cells increases with the highest concentration of nanoparticle, verifying the results obtained for the cytotoxicity studies. Additionally, the number of cells decreases significantly compared to the control, which may be caused by a loss of cells during the washes in the staining procedure.

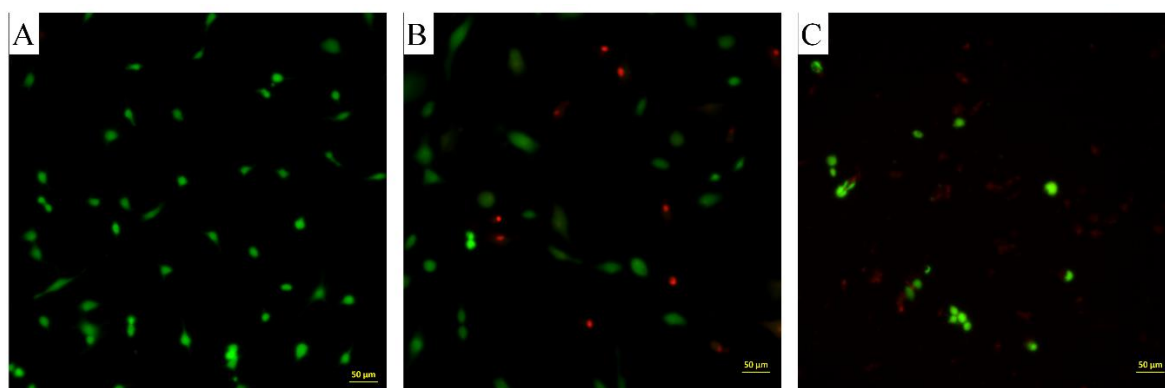


Figure 5.7. 785 nm laser treatment of glioblastoma cells for 15 minutes with (A) absence of nanoparticles, (B) 15 $\mu\text{g mL}^{-1}$ and (C) 20 $\mu\text{g mL}^{-1}$.

To quantify the percentage of cell mortality and the effectiveness of post-irradiation at 785 nm, the cells were incubated at different concentration of nanoparticles and irradiated over different periods of time (Fig. 5.8).

As it can be observed in Figure 5.8.A, the cell viability decreases accordingly when the nanoparticle concentration increases, showing the lowest values for 75 and 100 $\mu\text{g mL}^{-1}$ ($p < 0.05$) with a decrease of approximately 50% of live cells. However, when irradiated cells are compared to non-irradiated cells incubated during same periods and same nanoparticle concentration, the percentage of cell viability is similar. This data suggests that the irradiation at 785 nm of glioblastoma cells previously treated with G-Au-Pt nanoparticles does not show any significant improvement in the anticancer properties of the nanoparticles. Additionally, glioblastoma cells were directly irradiated at the same wavelength to ensure that the irradiation does not kill the cells directly (Fig. 5.8.B). The obtained results show that the number of live cells maintain the same value in all the periods from 5 to 5 min of irradiation as that of the control.

Previous data confirm that G-Au/Pt nanoparticles are not excited at 785 nm, so that the release of heat by irradiation is invalid at this wavelength. Moreover, in order to improve the efficacy of this treatment, the laser chosen would need to have an excitation wavelength within the range of absorption, which in this case of these nanoparticles is between 500 and 600 nm.

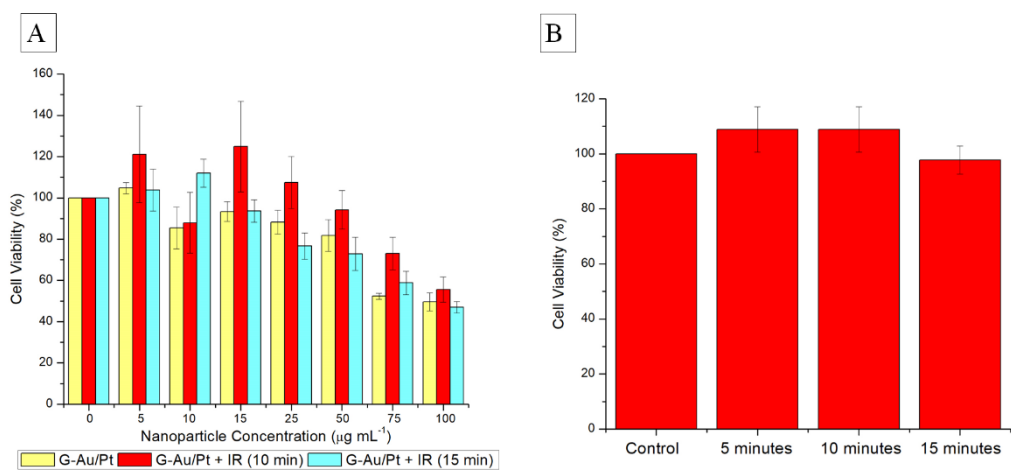


Figure 5.8. (A) Viability percentage of glioblastoma cells incubated with nanoparticles and irradiated. (B) Viability percentage of cell at different periods of irradiation.

6. Conclusions and future prospects

6.1. Conclusions

First, two types of bimetallic nanoparticles have been successfully synthesized via mediated human glioblastoma cells as a contribution to the green synthesis, and characterized by UV-visible spectroscopy, phase contrast microscopy, transmission electron microscopy and electron-dispersive X-ray spectroscopy. An ethanol treatment was then carried out to enhance the release of bimetallic nanoparticles from the cellular matrix that remain in the sample, showing no significant results.

Second, the synthesized nanoparticles were tested in glioblastoma cells to evaluate their effectiveness as anticancer agents, and in human dermal fibroblasts to study their biocompatibility in healthy human cells. The nanoparticles were analyzed before and after the ethanol treatment, showing a decrease in the anticancer activity after this treatment and no effect on the biocompatibility. Additionally, the number of reactive oxygen species was collected as marker of the anticancer activity in glioblastoma cells, with good results in case of G-Au/Pt nanoparticles.

Finally, the synthesized G-Au/Pt nanoparticles were used in photothermal therapy to kill glioblastoma cells. The application of irradiation technique at 785 nm did not show any enhancement in the cell mortality, due to a lack of excitation of the metal nanoparticles at this wavelength.

6.2. Future prospects

As a next step, the main objective is to enhance the purification process of the synthesized bimetallic nanoparticles using alternative techniques, such as ultrasonication.

Another goal is to improve the photothermal therapy technique by changing the irradiation wavelength to one within the range of absorption of G-Au/Pt nanoparticles. Alternatively, the nanoparticle surface can be functionalized with biomolecules capable of absorbing at this wavelength with the aim to increase the efficacy of this treatment.

Finally, the last goal will be to study, design and synthesize of drug carriers, such as liposomes, with the ability to cross the blood brain barrier (BBB) and release the bimetallic nanoparticles in the localized tumor.

7. References

1. GM, C. *The Cell: A Molecular Approach. 2nd edition.* (ASM Press, 2000).
2. Davis, M. E. Glioblastoma: Overview of Disease and Treatment. *Clin J Oncol Nurs* **20**, 1–14 (2016).
3. <https://emedicine.medscape.com/article/340870-overview>. 07/06/2018
4. <https://www.proteinatlas.org/learn/dictionary/pathology/glioma+3/detail+1/magnification+1>.
5. Siegel, R. L., Miller, K. D. & Jemal, A. Cancer Statistics , 2016. *CA Cancer J Clin* **66**, 7–30 (2016).
6. Gilbert, E. S. Ionizing Radiation and Cancer Risks: What Have We Learned From Epidemiology? *Int J Radiat Biol* **85**, 467–482 (2010).
7. Agency, I. & Monographs, I. Carcinogenicity of some industrial chemicals. **17**, 419–420 (2016).
8. Hemminki, K. & Pershagen, G. Cancer Risk of Air Pollution: Epidemiological Evidence. *Environ. Health Perspect.* **102**, 187–192 (1994).
9. Furrukh, M. Tobacco Smoking and Lung Cancer. *SQU Med. J.* **13**, 345–358 (2013).
10. Boffetta, P. & Nyberg, F. Contribution of environmental factors to cancer risk. *Br. Med. Bull.* **68**, 71–94 (2018).

11. Sudhakar, A. History of Cancer, Ancient and Modern Treatment Methods. *J Cancer Sci Ther* **1**, 1–4 (2009).
12. Hamilton, W. Cancer diagnosis in primary care. *Br. J. Gen. Pract.* **60**, 121–127 (2010).
13. Sudhakar, a. History of Cancer, Ancient and Modern Treatment Methods Akulapalli. *J Cancer Sci Ther.* **1**, 1–4 (2010).
14. Shewach, D. S. & Kuchta, R. D. Introduction to cancer chemotherapeutics. *Chem. Rev.* **109**, 2859–2861 (2009).
15. Shaloam Dasari and Paul Bernard Tchounwou. Cisplatin in cancer therapy: molecular mechanisms of action. *Eur J Pharmacol* **5**, 364–378 (2015).
16. Housman, G. *et al.* Drug resistance in cancer: An overview. *Cancers (Basel)*. **6**, 1769–1792 (2014).
17. Baskar, R., Lee, K. A., Yeo, R. & Yeoh, K. W. Cancer and radiation therapy: Current advances and future directions. *Int. J. Med. Sci.* **9**, 193–199 (2012).
18. Ramirez, L. Y. *et al.* Potential Chemotherapy Side Effects: What Do Oncologists Tell Parents? *Pediatr Blood Cancer* **52**, 497–502 (2009).
19. Corrie, P. G. Cytotoxic chemotherapy: Clinical Aspects. *Med.* **36**, 24–28 (2007).
20. http://www.softschools.com/formulas/chemistry/cisplatin_formula/446/.
21. <https://www.mayoclinic.org/tests-procedures/radiation-therapy/about/pac-20385162>.

22. McCune, J. S. Immunotherapy to Treat Cancer. *Clin. Pharmacol. Ther.* **100**, 198–203 (2016).
23. Behrouzkia, Z., Joveini, Z., Keshavarzi, B., Eyvazzadeh, N. & Aghdam, R. Z. Hyperthermia: How can it be used? *Oman Med. J.* **31**, 89–97 (2016).
24. Emdad, L., Sarkar, D. & Fisher, P. B. Gene Therapies for Cancer: Strategies, Challenges and Successes. *HHS Public Access* **230**, 259–271 (2016).
25. Maeda, H. The enhanced permeability and retention (EPR) effect in tumor vasculature: The key role of tumor-selective macromolecular drug targeting. *Adv. Enzyme Regul.* **41**, 189–207 (2001).
26. Baptista, P. Noble Metal Nanoparticles Applications in Cancer. *J. Drug Deliv.* **2012**, 1–12 (2012).
27. Huang, X. & El-Sayed, M. A. Gold nanoparticles: Optical properties and implementations in cancer diagnosis and photothermal therapy. *J. Adv. Res.* **1**, 13–28 (2010).
28. Qin, B. *et al.* Structure and characterization of TeO₂ nanoparticles prepared in acid medium. *Mater. Lett.* **63**, 1949–1951 (2009).
29. Shim, K., Kim, J., Heo, Y., Jiang, B. & Li, C. Synthesis and Cytotoxicity of Dendritic Platinum Nanoparticles with HEK-293 Cells. *Chem Asian J.* **350**, 21–26 (2017).
30. Buzea, C., Pacheco, I. I. & Robbie, K. Nanomaterials and nanoparticles: Sources and toxicity. *Biointerphases* **2**, MR17-MR71 (2007).

31. Links, D. A. Green Chemistry Green synthesis of metal nanoparticles using plants. *Green Chem.* **13**, 2638–2650 (2011).
32. Philip, D. Green synthesis of gold and silver nanoparticles using Hibiscus rosa sinensis. *Phys. E Low-dimensional Syst. Nanostructures* **42**, 1417–1424 (2010).
33. Nadagouda, M. N. & Varma, R. S. Green synthesis of silver and palladium nanoparticles at room temperature using coffee and tea extract. 859–862 (2008). doi:10.1039/b804703k
34. Kouvaris, Pantelis, et al. Green Synthesis and Characterization of Silver Nanoparticles Produced Using Arbutus Unedo Leaf Extract. *Mater. Lett.* **76**, 18–20 (2012).
35. Cruz, D. M., Mi, G. & Webster, T. J. Synthesis and characterization of biogenic selenium nanoparticles with antimicrobial properties made by Staphylococcus aureus , methicillin-resistant Staphylococcus aureus (MRSA), Escherichia coli , and Pseudomonas aeruginosa. *J. Biomed. Mater. Res. A* 1400–1412 (2018). doi:10.1002/jbm.a.36347
36. Klaus, T., Joerger, R. & Olsson, E. Silver-based crystalline nanoparticles microbially fabricated. *PNAS* **96**, 13611–13614 (1999).
37. Fayaz, A. M. et al. Biogenic synthesis of silver nanoparticles and their synergistic effect with antibiotics : a study against gram-positive and gram-negative bacteria. *Nanomedicine Nanotechnology, Biol. Med.* **6**, 103–109 (2010).
38. Venkataraman, J. S. et al. Growth of Gold Nanoparticles in Human Cells. *Langmuir* 11562–11567 (2005).

39. El-said, W. A., Cho, H., Yea, C. & Choi, J. Synthesis of Metal Nanoparticles Inside Living Human Cells Based on the Intracellular Formation Process. *Adv. Mater.* **26**, 910–918 (2014).
40. Miller, D. M., Buettner, G. R. & Aust, S. D. Transition metals as catalysts of ‘autoxidation’ reactions. *Free Radic. Biol. Med.* **8**, 95–108 (1990).
41. Song, W. *et al.* Role of the dissolved zinc ion and reactive oxygen species in cytotoxicity of ZnO nanoparticles. *Toxicol. Lett.* **199**, 389–397 (2010).
42. Devasagayam, T. P. A., Tilak, J. C., Bloor, K. K. & Sane, K. S. Free Radicals and Antioxidants in Human Health: Current Status and Future Prospects. *J Assoc Physicians India* **52**, 794–804 (2004).
43. Wang, H. *et al.* Targeted production of reactive oxygen species in mitochondria to overcome cancer drug resistance. *Nat. Commun.* **9**, (2018).
44. Aioub, M., Panikkanvalappil, S. R. & El-Sayed, M. A. Platinum-Coated Gold Nanorods: Efficient Reactive Oxygen Scavengers That Prevent Oxidative Damage toward Healthy, Untreated Cells during Plasmonic Photothermal Therapy. *ACS Nano* **11**, 579–586 (2017).
45. Ghosh, S. *et al.* Increased heating efficiency and selective thermal ablation of malignant tissue with DNA-encased multiwalled carbon nanotubes. *ACS Nano* **3**, 2667–2673 (2009).
46. Turkevich, J., Stevenson, P. C. & Hillier, J. A Study of the Nucleation and Growth Processes in the Synthesis of Colloidal Gold. *Discuss Faraday Soc* **11**, 55–75 (1951).

47. Nadagouda, M. N. *et al.* Synthesis of silver and gold nanoparticles using antioxidants from blackberry, blueberry, pomegranate, and turmeric extracts. *ACS Sustain. Chem. Eng.* **2**, 1717–1723 (2014).
48. Kajani, A. A., Bordbar, A., Hamid, S., Esfahani, Z. & Razmjou, A. RSC Advances Gold nanoparticles as potent anticancer agent: *RSC Adv* **6**, 63973–63983 (2016).
49. Teow, Y. & Valiyaveetil, S. Active targeting of cancer cells using folic acid-conjugated platinum nanoparticles. *Nanoscale* **2**, 2607–2613 (2010).
50. Alshatwi, A. A., Athinarayanan, J. & Periasamy, V. S. Green synthesis of bimetallic Au@Pt nanostructures and their application for proliferation inhibition and apoptosis induction in human cervical cancer cell. *J. Mater. Sci. Mater. Med.* **26**, (2015).
51. Dutta, D., Chattopadhyay, A. & Ghosh, S. S. Cationic BSA Templated Au-Ag Bimetallic Nanoclusters As a Theranostic Gene Delivery Vector for HeLa Cancer Cells. *ACS Biomater. Sci. Eng.* **2**, 2090–2098 (2016).
52. Huang, X., El-Sayed, I. H., Qian, W. & El-Sayed, M. A. Cancer cell imaging and photothermal therapy in the near-infrared region by using gold nanorods. *J. Am. Chem. Soc.* **128**, 2115–2120 (2006).
53. Tang, S., Chen, M. & Zheng, N. Sub-10-nm Pd nanosheets with renal clearance for efficient near-infrared photothermal cancer therapy. *Small* **10**, 3139–3144 (2014).
54. McGrath, A. J. *et al.* Gold over Branched Palladium Nanostructures for Photothermal Cancer Therapy. *ACS Nano* **9**, 12283–12291 (2015).

55. Alshatwi, A. A., Athinarayanan, J. & Vaiyapuri Subbarayan, P. Green synthesis of platinum nanoparticles that induce cell death and G2/M-phase cell cycle arrest in human cervical cancer cells. *J. Mater. Sci. Mater. Med.* **26**, 1–9 (2015).